Energies **2014**, *7*, 4068-4086; doi:10.3390/en7074068

OPEN ACCESS

energies

ISSN 1996-1073

www.mdpi.com/journal/energies

Article

The Marsili Volcanic Seamount (Southern Tyrrhenian Sea): A Potential Offshore Geothermal Resource

Francesco Italiano [1,*], Angelo De Santis [2], Paolo Favali [2], Mario Luigi Rainone [3], Sergio Rusi [3] and Patrizio Signanini [3]

[1] Istituto Nazionale di Geofisica e Vulcanologia-via Ugo La Malfa 153, 90146 Palermo, Italy

[2] Istituto Nazionale di Geofisica e Vulcanologia-via di Vigna Murata, 605, 00143 Roma, Italy; E-Mails: angelo.desantis@ingv.it (A.D.S.); paolo.favali@ingv.it (P.F.)

[3] Dipartimento di Ingegneria e Geologia-Università "G. d'Annunzio", 66100 Chieti, Italy; E-Mails: rainone@unich.it (M.L.R.); s.rusi@unich.it (S.R.); signanini@unich.it (P.S.)

* Author to whom correspondence should be addressed; E-Mail: francesco.italiano@ingv.it; Tel.: +39-091-680-9411; Fax: +39-091-689-0965.

Received: 18 April 2014; in revised form: 9 June 2014 / Accepted: 10 June 2014 / Published: 26 June 2014

Abstract: Italy has a strong geothermal potential for power generation, although, at present, the only two geothermal fields being exploited are Larderello-Travale/Radicondoli and Mt. Amiata in the Tyrrhenian pre-Apennine volcanic district of Southern Tuscany. A new target for geothermal exploration and exploitation in Italy is represented by the Southern Tyrrhenian submarine volcanic district, a geologically young basin (Upper Pliocene-Pleistocene) characterised by tectonic extension where many seamounts have developed. Heat-flow data from that area show significant anomalies comparable to those of onshore geothermal fields. Fractured basaltic rocks facilitate seawater infiltration and circulation of hot water chemically altered by rock/water interactions, as shown by the widespread presence of hydrothermal deposits. The persistence of active hydrothermal activity is consistently shown by many different sources of evidence, including: heat-flow data, gravity and magnetic anomalies, widespread presence of hydrothermal-derived gases (CO_2, CO, CH_4), $^3He/^4He$ isotopic ratios, as well as broadband OBS/H seismological information, which demonstrates persistence of volcano-tectonic events and High Frequency Tremor (HFT). The Marsili and Tyrrhenian seamounts are thus an important—and likely long-lasting-renewable energy resource. This raises the possibility of future development of the world's first offshore geothermal power plant.

Keywords: geothermal energy exploration; Italy; Marsili; volcanic seamount; offshore

1. Introduction

A large amount of data on the geological, geophysical and geochemical features of submarine volcanic activity and seamounts have been acquired in the last three decades. The close proximity of magma chambers to the seafloor, in conjunction with tectonic activity due to plate motion, deformation and cooling of erupted lavas results in convective circulation of dense, cold seawater through the cracked and fissured upper portions of the lithosphere; this circulation promotes the formation of venting sites that release hot hydrothermal fluids and dissolved elements [1–4].

Submarine hydrothermal activity has been studied so far as an energy source for free-living and symbiotic chemosynthetic bacteria, which form the base of the food chain in these unique habitats [5]. Because of their huge, long-lasting recharge and high-temperature/high-pressure characteristics, the submarine hydrothermal fluids are now investigated also as a potentially exploitable geothermal energy source. Candidate areas for offshore geothermal exploitation have been identified in the Gulf of California, the Juan de Fuca Ridge, the Japan Sea, the Okhotsk Sea, the Andaman Sea and the Tyrrhenian Sea since late 1970s [6]. However, the technology at that time was not still achievable at competitive costs beyond environmental, legal and institutional problems which had to be overcome. Nowadays, the continuous and growing developments in oil and gas exploration and exploitation techniques allow for an easier and economically competitive approach to the investigation and the energy potential assessment of submarine hydrothermal systems. However, before any reliable quantification for energetic exploitation of any offshore geothermal reservoir, a multidisciplinary submarine exploration has to be done, including geological, geophysical geochemical, oceanographic and biological investigations.

At the beginning of the last century, Italy became the first country worldwide to exploit high-temperature geothermal resources for power generation, with the result that, nowadays, Larderello-Travale/Radicondoli and Mt. Amiata (Bagnore and Piancastagnaio) are exploited geothermal fields [7]. They are both set in a continental extensional tectonic environment (lithospheric thickness between 20 and 30 km), characterised by deep and shallow volcanic systems and high heat-flow values (regional value of 120 mW/m^2, with maxima up to 1 W/m^2 [8]). In both the geothermal areas, magmatic bodies provide the necessary heat source to deep and shallow reservoirs hosted in local metamorphic, carbonate and anhydritic formations [9,10]. In order to improve the Italian geothermal energy production, in 1970s and 1980s an intensive exploration program (geological, geophysical and geochemical surveys, as well as drilling activities) took place in Latium (about 100-deep wells were drilled in the Latera caldera, Vico Lake, Cesano, Bracciano Lake and Alban Hills), Campania (Phlaegrean Fields and Ischia Island) and Sicily (Vulcano and Pantelleria Islands) [7]. Several unfavourable physical, chemical and logistic features strongly limited the use of these potential geothermal fields. In particular, the geothermal exploitation was hindered by the low permeability of the reservoirs, the high salinity and acidity of the hot fluids, the sluggish and low amount of groundwater

recharge, the high potential explosivity of these magmas (rhyolites, trachytes and phonolites) implying a high volcanic hazard as well as the strong urbanisation and/or tourist use of those areas.

The Southern Tyrrhenian Sea might represent the future target for geothermal energy exploration and exploitation due to the generally high heat-flow [11,12] and the widespread presence of seamounts for which the presence of hydrothermal deposits has been well documented. Among them, the Marsili seamount exhibits some features that make it a potential site hosting exploitable submarine geothermal systems.

This paper accounts for the recently collected information of geological, geochemical and geophysical features of the Marsili seamount (Figure 1), the largest European and Mediterranean volcanic edifice, making the seamount a likely large geothermal energy resource that could significantly improve the Italian geothermal power generation, nowadays providing 5.5 TWh per year that cover only 1.6% of national mean electricity production [13].

Figure 1. Location of the study area. MV: Marsili Volcano; MB Marsili Basin; ST: volcanoes of Stromboli; VU: volcanoes of Vulcano; FL: Filicudi Island; SIS: Sisifo submarine Volcanoes; LM: Lametini Seamounts; PA: Palinuro Seamount; VB: Vavilov Basin. The map on the right is modified after [14].

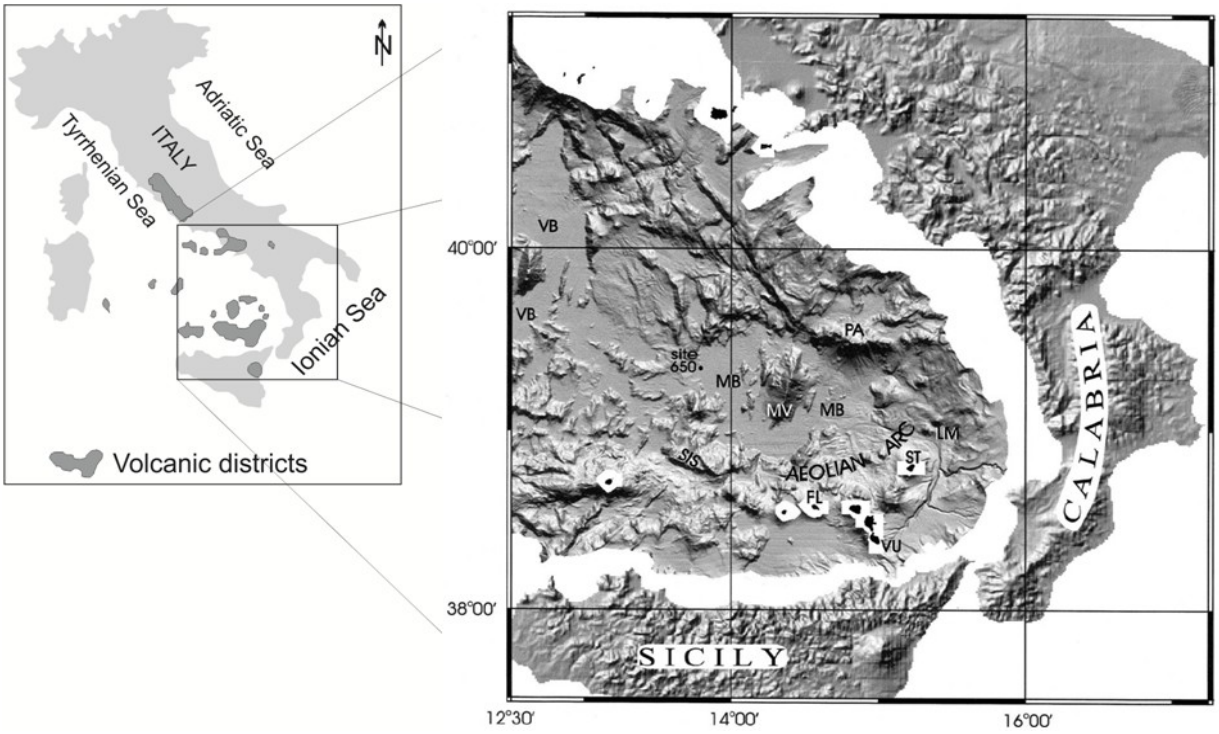

2. Results

This section summarizes the results of a large number of multidisciplinary data collected by several scientific cruises carried out by Italian Research Institutions during the last 20 years and describes the new results collected during two campaigns carried out in 2007 and 2010.

2.1. Geothermal Potential of Southern Tyrrhenian Basin and Marsili Seamount

The Southern Tyrrhenian Sea is a back-arc basin developed from Miocene to Present in the frame of the coeval formation of Apennine-Maghrebides chain, structured above the subducting north-western Ionian oceanic slab [15,16]. Its evolution has been characterised by volcanic activity induced by a wide tectonic extension from North-West (Sardinia) to South-East (Aeolian Arc) [17–19]; deep and shallow seismicity occurring in this area has been also well documented (e.g., [20–22]). The best morphologic evidences of these geodynamic processes are the two oceanic crust floored Vavilov and Marsili sub-basins and the homonymous seamounts, placed at north-west and south-east portions of the Southern Tyrrhenian basin, respectively [14,23]. Other geodynamic-related morphologic features are the numerous volcanic structures forming an arc all along the south-eastern margin of the basin: the Aeolian Arc, representing the emerged part; Palinuro, Glabro, Alcione and Lametini, representing the northern submerged arm; Eolo, Enarete and Sisifo, representing the north-western submerged arm (Figure 2; [23]).

Figure 2. Bathymetry of South-Eastern Tyrrhenian Basin. M: Marsili; MB: Marsili Basin; P: Palinuro; A: Alcione; L: Lametini; Sc: Stromboli Canyon; Eo: Eolo; En: Enarete; S: Sisifo (modified after [23]).

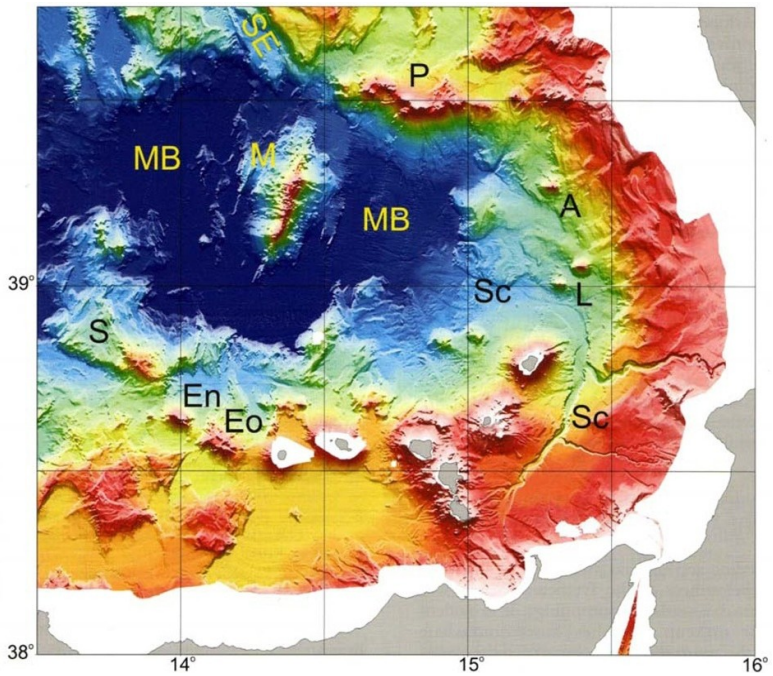

The heat-flow anomalies of Southern Tyrrhenian Sea [11,12] are always high in correspondence with the volcanic structures; the regional mean value is higher than 120 mW/m^2 and comparable to the Italian onshore volcanic district. More precisely, the highest values have been recorded close to the Vavilov (140 mW/m^2) and Marsili (250 mW/m^2) seamounts. Heat-flow rates as high as 300 mW/m^2 and 500 mW/m^2 were detected on the uppermost and central portion of Vavilov and Marsili seamounts respectively [24]. Those values fit with the geophysical data, collected in the last decades such as:

- Moho depth located 15–20 km below the Tyrrhenian abyssal plains and about 10 km beneath Vavilov and Marsili sub-basins [25,26];

- Gravity anomalies with positive values greater than 250 mGals, interpreted as due to lithosphere thinning [27], as well evidenced by high resolution reflection seismic profiles [28];
- A lithosphere mean conductivity beneath Marsili basin about one order of magnitude greater than beneath Ustica island (South-western Tyrrhenian basin) [29].

All the above-mentioned data strongly suggest the following inferences:

- Southern Tyrrhenian basin is affected by numerous and distributed heat sources, generally represented by hot magmatic bodies at shallow depths (<10 km) in a strong extensional geodynamic setting;
- A high primary permeability field is inferred, due to emplacement and cooling of magmas, successively increased by the intense and recent tectonic activity [30,31];
- A virtually infinite fluid recharge is available, supplied by pressurised seawater;
- A relatively low amount of dissolved salts with mild acidity is expected;
- A low explosivity due to the presence of lesser involved magmas with a lower amount of dissolved water is expected.

In this frame, Marsili seamount, presenting the highest aforementioned anomalies, is here proposed as the best prone site of sustained submarine geothermal potential. Marsili seamount is a recent volcanic structure (1–0.1 Ma), mainly composed of basalts and, to a lesser extent, andesites and trachy-andesites with calc-alkaline affinity [32–34]. This structure has been interpreted as an inflated, small-scale spreading centre, since bio- and magneto-stratigraphic data show features comparable to those typical of mid-ocean ridges [35–38].

Dekov and Savelli [39], summarising all the observations since the late 1960s on the rocks sampled from Marsili and surrounding volcanic centres, affirmed that these areas are affected by hydrothermal fluid circulation; in their model, cold seawater enters into fractured rocks and then is superheated by magmatic bodies at crustal depths. Clues of active venting of hydrothermal fluids over the Marsili seamount have been provided by the injection of magmatic-type volatiles into the sea water as demonstrated by the anomalous ^{3}He content and the whole chemical composition of the gases dissolved in water column [40]. However, direct thermal measurements on Marsili seamount are still lacking. This latter discovery strongly points to Marsili still being hydrothermally active, in agreement with the previous mineralogical data, and supported by a significant contribution by juvenile fluids.

2.2. Morphology

The physiographic features of Marsili seamount are shown in Figure 3. The Marsili seamount rises 3500 m from the abyssal plain to 489 m minimum depth. The volcanic edifice is about 60 km long and about 20 km wide; two other smaller structures run parallel to the volcano and are located on its left and right part, with heights on the order of several hundred metres. Marsili is elongated mainly along a NNE-SSW axis; however, this extensional axis is not perfectly linear but it shows a sigmoid trend, with the southernmost and northernmost axial directions both north-eastern trending, while the central axis is closer to the N-S direction. This deformational feature is commonly associated with strike-slip faulting under volcanoes [41], but it can also be related to long kilometric normal faults orthogonal to the volcanic system spreading direction, with transverse faults at the tips that accommodate the

regional strain [42]. In both cases, this observation implies a strong tectonic control of the whole volcanic edifice. The volcano summit is characterised by a narrow crest, 20 km long and 1-km wide, over the 1000 m isobaths, cut by linear structures, mainly disposed parallel to the extensional axis. They appear as small ridges, up to 100 m high and 750 m long, not fault bounded, formed by alignments of small monogenic volcanic mounds. These segments may result from the feeding of magma to the seafloor along dikes that produce, or follow, discontinuous, en-echelon crack systems. Steep bathymetric gradients separate the crest portions from the deeper volcano flanks, forming very long and lesser sloped scarps extending to the basin. In several places, these lower steep scarps terminate with gently dipping terraces, elevated for several hundreds of meters from the abyssal Marsili basin. Spherical cones are present on the flanks of the volcano with diameters ranging between a few kilometres to several hundred metres.

These flanks are also cut by several, well evidenced kilometric valleys; the largest of them is located near to the central and top portion of Marsili. It has an amphitheatre shape in the uppermost part edged by roughly vertical walls; such geomorphologic feature suggests a flank collapse of this portion of the Marsili flank, with landslide debris accumulated distally on the Marsili basin, a kind of process already found elsewhere [43,44].

Figure 3. Detailed bathymetry of Marsili seamount. Red dashed lines: linear structures; violet dotted lines: main circular cones and terraces; yellow dashed line: major landslide (modified after [45]).

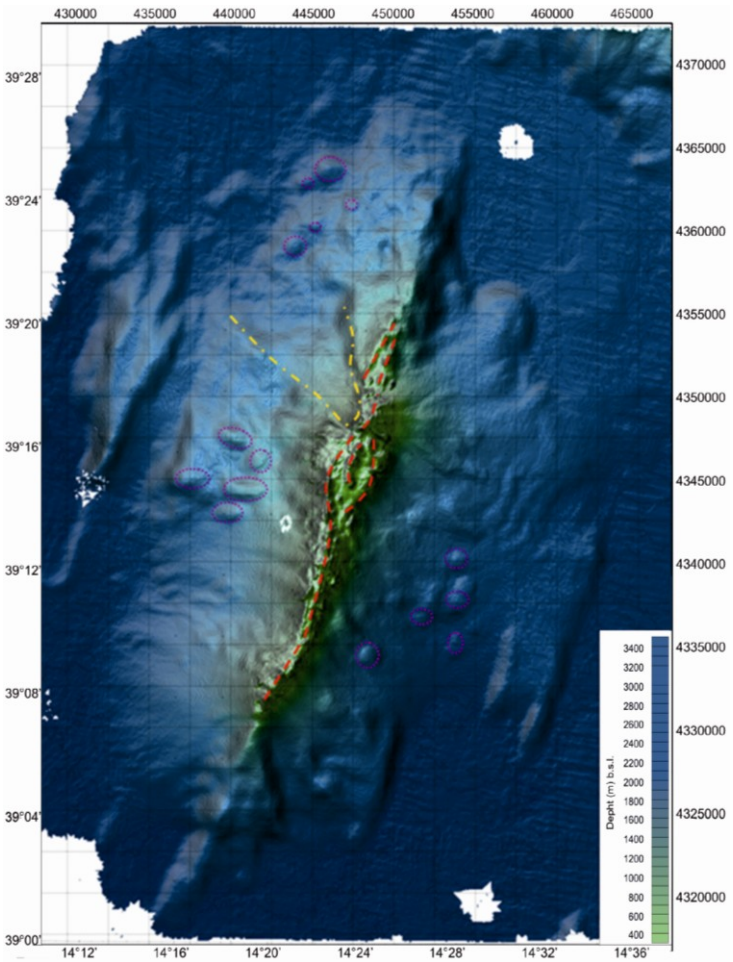

2.3. Magnetic Data

Figure 4 shows the total field magnetic anomaly map, reduced to the magnetic pole, recorded above Marsili seamount. In agreement with literature data [35,37,38], positive magnetic anomaly maxima are located along the central sectors of the volcanic structure. At northern and southern tips the highest positive anomalies of Marsili are present, with maximum values around 1500 nT; in the central and highest portion of volcano and in the middle of these two former anomalies, the values are around 0 nT, reaching a minimum of −100 nT. Negative anomalies are located at the base of the western flank, with a mean value around −200 nT; the base of the eastern flank again shows negative values, achieving a local minimum of −500 nT in the central and southern portions, whereas the north-eastern part of this sector is characterised by small positive values.

Figure 4. Magnetic anomaly field (reduced to magnetic pole) of Marsili; values of the magnetic anomaly field in nT (modified after [45]).

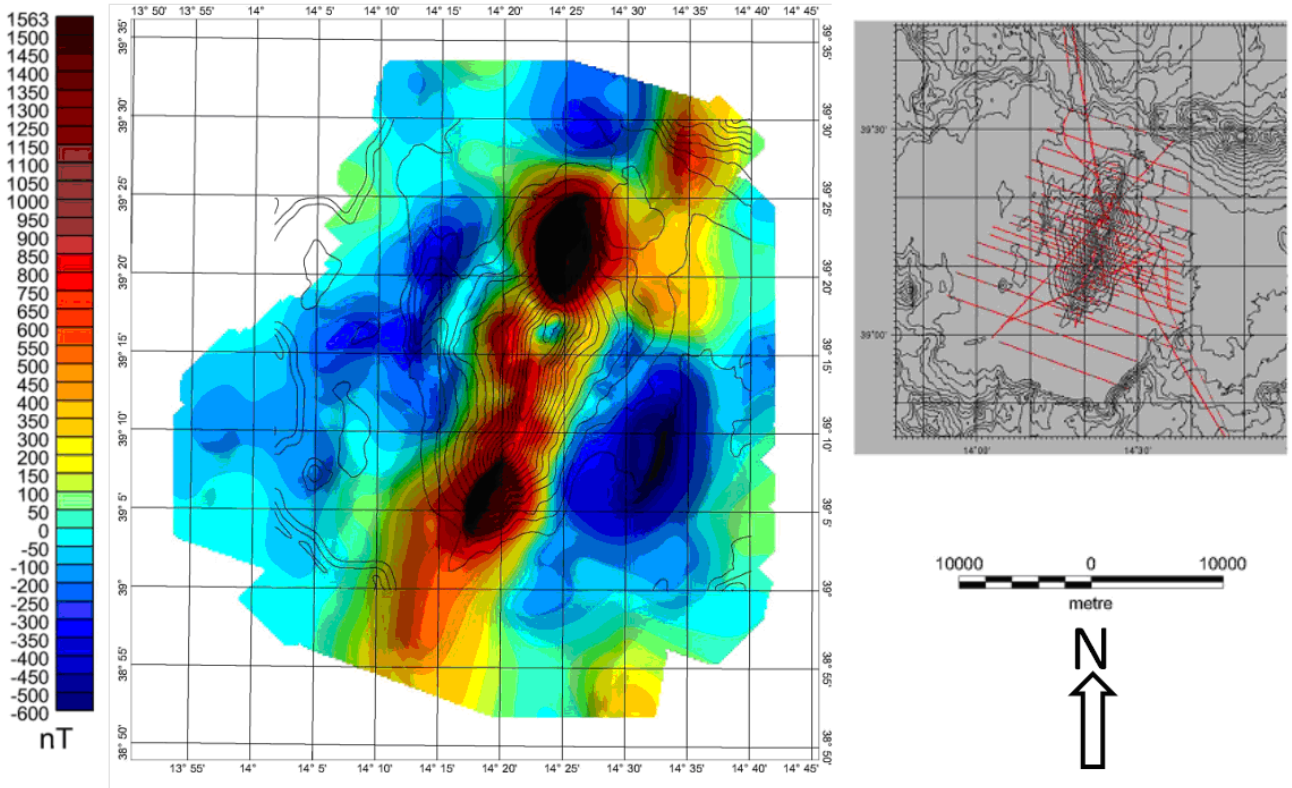

2.4. Gravity Data

According to the map of Faye gravity anomalies of Marsili seamount (Figure 5), positive maxima, reaching more than 80 mGals, are present on the crest portion of volcano, above the 1000 m isobaths, and progressively decrease to about 20 mGals on the volcano base. On the whole, the sea-surface free-air anomaly field largely reflects the topography of the volcano; moreover, the relative low amplitude of the positive gravity anomalies suggests the presence of a low density zone below the seamount.

2.5. Seismological Recordings

The broadband OBS/H (Ocean Bottom Seismometer with Hydrophone), deployed on the Marsili flat top (39°16,383', 14°23,588') at a depth of 790 m, recorded more than 1000 seismo-volcanic and hydrothermal signals [3]. By comparing the signals recorded with typical volcanic seismic activity, the recorded signals were grouped into: Volcano-Tectonic type A (1 event), Volcano-Tectonic type B (817 event), High Frequency Tremor (159 events) and quasi-monochromatic Short Duration Events (32 event).

Figure 5. Faye anomaly field of Marsili seamount; values of the gravity field in mGal (modified after [45]).

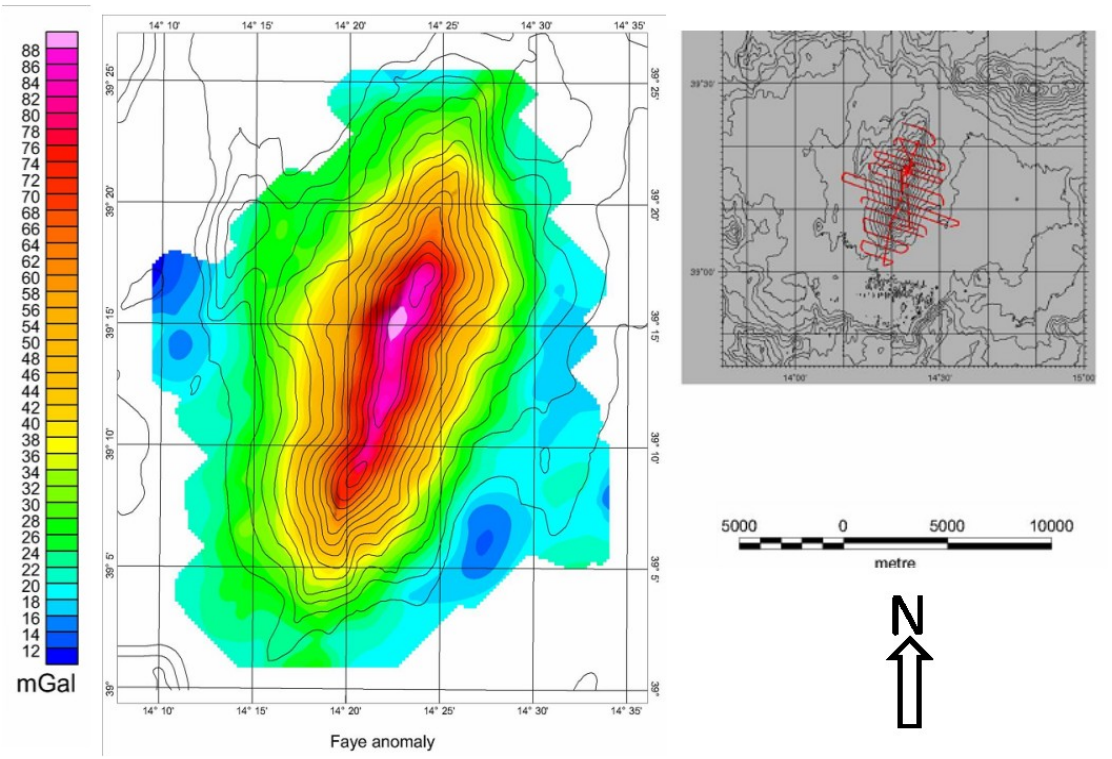

An intriguing feature of the seismic noise is its spectral content presenting progressively growing energy levels in a broad-band frequency range from 4 to 60 Hz; diffuse spectral peaks are also present between 4 and 30 Hz. The seismic events are characterized by an indiscernible S-phase. On the basis of preliminary frequency content observations they can be distinguished in two main groups: about 720 events with frequency content between 4 and 10 Hz and about 80 events with very high frequency content, between 40 and 80 Hz [3].

2.6. Hydrothermal Fluids

In order to recover information on the type of vented fluids and to constrain their origin, we carried out water column surveys performing casts and tows across the seamount using a rosette equipped with a CDT (SeaBird 911+ Conductivity Temperature Depth device) and Niskin bottles. The surveys have been carried out during two scientific cruises in November 2007 (by R/V Urania) and July 2010 (by R/V Astrea).

Sea-water samples were collected to extract the dissolved gas phase by further laboratory procedures. The extracted gases were analyzed for the chemical composition calculated taking into account the solubility coefficients (Bunsen coefficients "β") of each gas specie, the volume of the gas extracted (in cm^3), the volume of the extracted water sample (in cm^3) and the equilibration temperature as described in [46,47].

Table 1 lists the results (expressed in cm^3 STP/L_{H2O}, namely millilitres of gas per litre of water at standard temperature and pressure conditions of 1bar and 25 °C) showing that CO_2, with concentrations ranging from 0.53 to 1.9 cm^3 STP/L_{H2O}, is by far the most abundant component of the dissolved gas phase besides oxygen and nitrogen, in the range 2.7–4 and 8.3–10 cm^3 STP/L_{H2O}, respectively. Among the other components CH_4 is always detected in concentrations ranging from 3.9×10^{-5} to 2.1×10^{-4} cm^3 STP/L_{H2O}, two orders of magnitude above the equilibrium with the atmosphere (ASSW value equal to 1×10^{-6} cm^3 STP/L_{H2O}).

Table 1. Analytical results of the dissolved gas phase in samples collected during two different cruises (2007 and 2011). Hydrothermal-derived gases are released besides components from the atmosphere. Analytical results in cm^3 STP/L_{H2O} (see text for details). Depth in meters. Bdl = below detection limits. Data of ASSW (Air Saturated Sea Water) and from the bottom sample of a vertical cast carried out over the Tyrrhenian Abyssal plain are reported for comparison. Coordinates are reported as they were collected during the cruises.

ID Sample	Depth	Date	Latitude	Longitude	H_2	O_2	N_2	CH_4	CO_2
Marsili									
M1	676	13 July 2011	39°16.840'	14°23.220'	3.7×10^{-4}	3.50	9.25	9.5×10^{-5}	0.77
M1	500	13 July 2011	39°16.840'	14°23.220'	3.1×10^{-3}	3.60	10.04	5.2×10^{-5}	1.07
M1	400	13 July 2011	39°16.840'	14°23.220'	1.2×10^{-3}	4.03	12.92	1.3×10^{-4}	0.60
M1	300	13 July 2011	39°16.840'	14°23.220'	-	2.99	9.61	1.5×10^{-4}	0.63
M2	668	13 July 2011	39°17.159'	14°23.410'	-	3.23	9.10	3.9×10^{-5}	0.53
M2	500	13 July 2011	39°17.159'	14°23.410'	2.0×10^{-3}	3.42	10.21	1.3×10^{-4}	1.26
M2	400	13 July 2011	39°17.159'	14°23.410'	-	2.78	9.01	2.1×10^{-4}	1.89
M2	300	13 July 2011	39°17.159'	14°23.410'	-	3.28	9.35	1.1×10^{-4}	1.72
M3	610	13 July 2011	39°16.799'	14°23.999'	2.5×10^{-4}	3.12	9.16	5.8×10^{-5}	2.71
M3	500	13 July 2011	39°16.799'	14°23.999'	1.3×10^{-4}	2.74	8.29	1.0×10^{-4}	0.57
M3	400	13 July 2011	39°16.799'	14°23.999'	-	3.34	9.61	1.1×10^{-4}	1.72
M4	673	13 July 2011	39°16.342'	14°23.196'	4.8×10^{-4}	2.97	10.15	9.7×10^{-5}	1.29
M4	500	13 July 2011	39°16.342'	14°23.196'	2.9×10^{-4}	3.31	9.89	9.4×10^{-5}	0.80
M4	400	13 July 2011	39°16.342'	14°23.196'	1.1×10^{-3}	3.46	10.39	8.4×10^{-5}	0.98
Tow-yow Marsili									
TY1	500	02 November 2007	39.28163°	14.38428°	bdl	2.42	7.77	2.1×10^{-4}	0.47
TY2	702	02 November 2007	39.28165°	14.38447°	bdl	2.98	8.80	3.3×10^{-4}	0.45
TY3	457	02 November 2007	39.28763°	14.42715°	bdl	3.26	9.16	2.2×10^{-4}	0.44
Data for comparison									
Vertical cast	3164	02 November 2007	39.40733°	14.51067°	bdl	2.47	8.42	4.4×10^{-5}	0.55
	400	02 November 2007	39.11475°	14.32298°	bdl	2.45	7.58	2.1×10^{-4}	0.43
ASSW	-	-	-	-	4.1×10^{-5}	4.80	9.60	1.0×10^{-6}	0.24

3. Discussion

The collected data provide the first useful information on the characterisation of this huge offshore structure that might be a potential site for offshore geothermal exploitation. The large variety of morphological forms, *i.e.*, linear structures, lava sheets, spherical cones, fault scarps and landslides, suggests that Marsili volcanic seamount has encompassed a long evolution, composed of different stages. The whole volcanic edifice shows evidence of mature volcanism, since almost all the volcanic forms look diffusely marked by further tectonics and erosion. The most mature forms, represented by circular cones and terraces, lava sheets, *etc.*, are predominantly located on the lower flanks of Marsili volcano; the youngest ones, typically represented by linear structures, are along the crest portion. Fault scarps are easily observable, pointing out the influence of tectonics on the whole edifice. As a consequence, the volcano likely has a well-developed network of fractures and cavities that play an important role in defining the permeability field of the volcano; these provide a pathway for the inflow of seawater and the consequent hydrothermal circulation and are primarily responsible for determining the magnitude of submarine geothermal resources.

The basaltic to basaltic-andesite rock compositions reported in [34] are in agreement with the strength of magnetic anomalies measured on the northern and southern portions of the Marsili volcanic edifice. Generally, freshly erupted basalts (also rapidly cooled) are strongly magnetic [48,49] because they have not been exposed to demagnetisation processes for a long time. However, the most intriguing feature of the magnetic anomaly field are the very low values in the central sector of the crest, testifying the presence of rocks with very low and/or a-magnetic properties, for which hydrothermal activity is considered as the main cause. The hydrothermal circulation of fluids may interact with the source rocks and reduce the magnetisation by breaking down the magnetic minerals [50,51]; this evidence corroborates with the occurrence of hydrothermal processes, possibly still active or recorded by geothermal deposits on the crest of Marsili volcano [39,52]. The pattern of the observed anomalies fits with a Curie isotherm mean depth located at around 4–5 km below Marsili crest, indicating a temperature of more than 600 °C at the volcano base and highlighting the possible presence of magmatic bodies. The high internal temperatures are also supported by the extremely high heat-flow measurements carried out on Marsili [11,24]. All those complementary data coherently suggest that Marsili seamount contains an intense and shallow heat source.

Although hydrothermal minerals are generally less dense than primary minerals, their effect on gravity is negligible. The free-air anomaly high observed on the top of Marsili seamount occurs over the topographic high over which the hydrothermal system is supposed to be located. So, the gravity anomalies are controlled by local geologic structure. Generally, the observed gravity anomaly field can be fitted only assuming a mean density of the Marsili volcanic structure of about 2 g/cm^3. Taking into account the petrographic features of Marsili rocks [34] as well as the magnetic data, such values can be attributed to rock porosity/permeability, possibly filled with aqueous and volatile phases. On this basis, it can be tentatively inferred that the Marsili volcano should have a significant porosity, possibly more than 10% by volume.

Caratori Tontini *et al.* [53] proposed a model for the volcano summit consisting of a large altered region, with a vanishing magnetisation of 0 A/m and a density of 2.0 g/cm^3, and an active, a-magnetic hot magma chamber 3 km below the summit, with density 2.3 g/cm^3 based on volatile concentrations [54].

Seismic observations by means of the OBS/H deployed on the crest of Marsili seamount [3] fit with the presence of active hydrothermal discharge highlighted by the geochemical features of the dissolved gases (Table 1). The continuous high frequency seismic and acoustic noise recorded on the Marsili crest is in agreement with historic seismic noise recordings in geothermal areas. In particular, very shallow hydrothermal manifestations (active venting sites) usually produce signals with maximum energy in the frequency band over 50 Hz [55–57], as observed on Marsili seamount.

Moreover, the seismicity characterised by a frequency content between 4 and 10 Hz could be connected to hydrothermal fluids circulation, in analogy with long-period (LP) events (e.g., [58–60]), while those with 40–80 Hz frequency content could be generated by surface degassing phenomena ([3] and references therein).The results of the chemical and isotopic analyses of gas extracted from the sampled sea-waters allow us to confirm the existence of a dissolved gas phase different from the atmospheric. The results clearly show that besides the expected atmospheric gases, a significant content of CO_2 marks all the gas samples. Figure 6 shows the contemporary presence of atmospheric components (represented by O_2 and N_2) as well as CO_2 typically originated by an endogenic source.

Figure 6. O_2-N_2-CO_2 ternary diagram. The samples plot on a straight mixing line between atmospheric components O_2 and N_2 and CO_2 typically of magmatic/hydrothermal origin The Air Saturated Sea Water mark (grey star, ASSW) indicates where dissolved gases in ASSW (air-saturated sea water) sea water plot. Blue triangles = samples from above the area marked by physical anomalies (see text); grey crosses = samples from a tow-yow across the seamount; black filled circles = samples from a vertical cast over the Tyrrhenian batial plain. The numbers indicate the sampling depths.

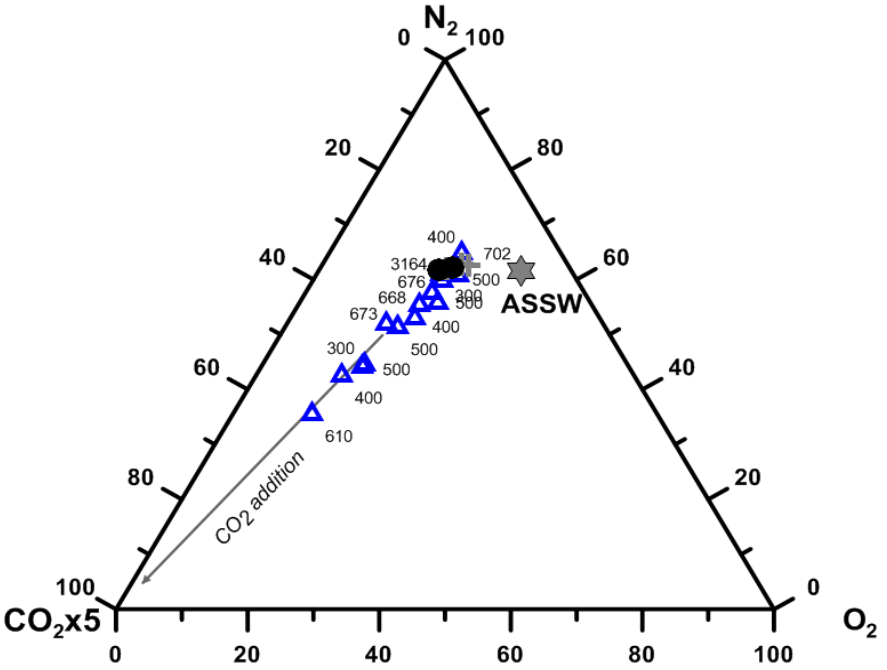

The plot along the Air-Saturated Sea Water (ASSW)-CO_2 mixing line highlights the injection of CO_2-dominated volatiles. Samples marked by the blue triangles come from the area marked by the largest anomalies of physical parameters (magnetic, gravimetric, seismic). Those samples plot along a line with a constant CO_2/N_2 ratio showing and increasing trend of hydrothermal fluids. Data from

waters sampled by a tow-yow across the whole seamount, show a lower, although significant CO_2 content, due to their provenance from other areas clearly marked by the presence of hydrothermal activity although of less intensity. Figure 7 plots atmospheric gas (typically represented by oxygen) together with CO_2 and CH_4 representative for hydrothermal-type components. The plot shows the occurrence of dissolution processes responsible for CO_2 loss and enhancement of the less soluble species such as CH_4. Both figures plot data collected during two cruises in 2007 (grey crosses) and 2011 (blue triangles). The latter samples have been collected over the area supposed to be the main geothermal source of the whole Marsili seamount where the low energy volcanic blasts might have occurred in recent times [61].

Figure 7. CH_4-O_2-CO_2 triangular diagram. The plot shows the relative concentrations of hydrothermal-derived components (CO_2-CH_4) besides the atmospheric component (here represented by oxygen) normally dissolved in sea water. It is easy to recognize the large enrichment in deep-originated CO_2 and CH_4 to the respect to ASSW. The arrows show the trends of modification of the dissolved gas assemblage due to the injection of hydrothermal fluids and the gas/water interaction phenomena leading to the dissolution of the very soluble CO_2 and enrichment of less soluble gas species like CH_4. Symbols as in Figure 6.

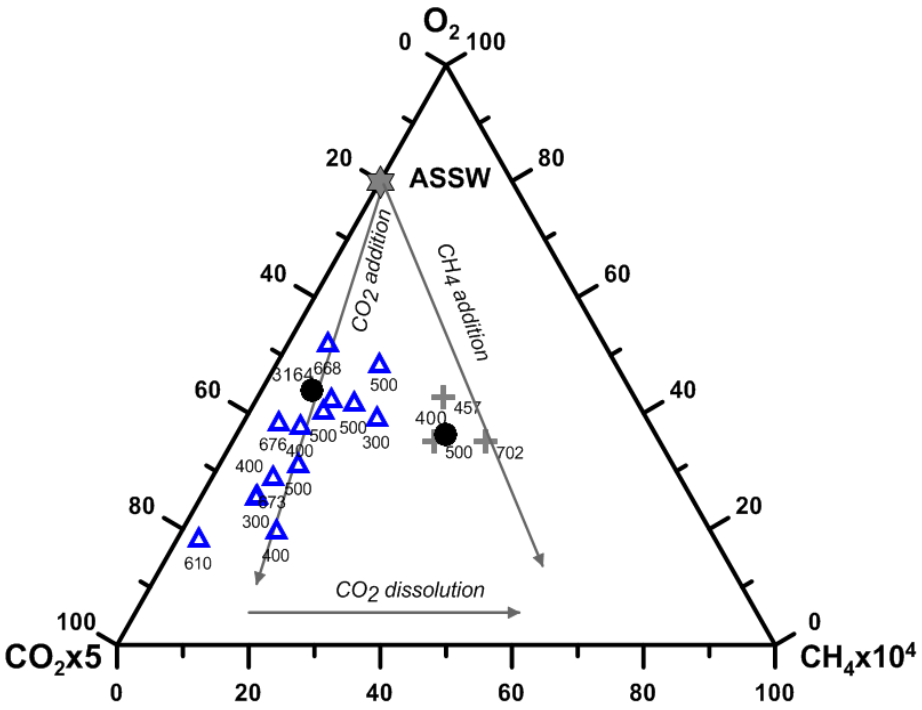

The available scientific data set has been considered a good starting point for an Italian company (Eurobuilding S.p.A., Servigliano, Italy) to propose a cutting-edge project to drill the first offshore geothermal well on the Marsili seamount, [62,63]. The estimates they performed bring to an effective electrical power generation of 200 MW. The offshore well should be connected to steam turbines that together with condenser systems, power generators and tension elevators could be hosted on the power plant platform. A high capacity cable will drive the electricity from the platform to the power grid located on the Italian coast.

4. Conclusions

The comprehensive and multidisciplinary (geological, geophysical and geochemical) dataset provided results coherently pointing to the Marsili seamount as a possible target for offshore geothermal exploration and exploitation developments.

The main scientific key points supporting future evaluations of the Marsili seamount as a possible geothermal energy resource can be summarized as:

(1) Marsili has a shallow and strong heat source;
(2) An active geothermal fluid circulation is expected as suggested by the first permeability field evaluations;
(3) The present state of Marsili volcanic activity is still controversial: recent radiometric data indicate the occurrence of recent magmatic blasts [61] although no indications come from other observations (e.g., seismic activity) and only sporadic monitoring activity has been carried out [64];
(4) The presence of solid deposits of hydrothermal origin indicates that geothermal fluids permeate the edifice and are vented into the seawater. The evidence that hydrothermal fluids as well as magmatic-type helium are injected in the deep sea waters indicates that the hydrothermal activity is still ongoing.

The possibility that a large geothermal energy reservoir exists about 100 km off the Italian coasts and that such a reservoir is able to provide a significant, long-lasting amount of exploitable energy, makes the Marsili seamount a potentially attractive target for private and public investors.

To summarize the case for developing the world's first offshore geothermal power plant in this region we consider a model of the edifice with constant average density of basalts equal to 2.67 g/cm^3, namely the difference between the gravimetric anomaly calculated from the model and that coming from the measurement leads to a density value between 1.7 and 2.3 g/cm^3. Considering also the petrologic and magnetic features of the rocks, the estimated density values can be a consequence of a high porosity of the rocks filled by volatiles. Assuming an average porosity of 10% and the total estimated volume of the geothermal reservoir >100 km^3, the volume of the geothermal fluids circulating in the central and upper part of the Marsili seamount, it results that about 10 km^3 of exploitable hot fluids can be recovered [45].

A first exploration drilling is needed to verify the proposed results and to recover (for the first time) direct information on the physical, chemical and isotopic features of the deep hydrothermal vents. In fact a hydrothermal fluid with a temperature of 250 °C and pressure of 30 bar with a flow rate of 1 m^3/s allows the energy production of 8 MW, while fluids marked by a temperature of 375 °C and pressure of 250 bar allow an energy production ten times bigger for the same flow rate.

It is absolutely clear that new data and further multidisciplinary investigations are needed, including the assessment of the natural risks (volcanic and seismic) related the huge and almost unknown submarine volcano. The development of micro-biological studies as well as research and development activities aimed at planning and deploying seafloor observatories for long-term monitoring activities [65] are also considered as mandatory. The results will improve the scientific knowledge useful to better constrain the available and exploitable geothermal resources inside the volcano. The future geothermal explorations have at least to include:

- The location of active venting sites and hydrothermal fluid release by direct (by ROVs) explorations and detailed CTD and nephelometry surveys;
- The distribution of the parameters that determine the permeability field of the volcano by geophysical tomographic methods;
- The characterization of volcanic-type ongoing processes, using seafloor observatories planned to carry out long-term monitoring of temporal variation of both physical and chemical parameters;
- The assessment of all the environmental aspects related to geothermal exploitation activities including studies to forecast and to face the impact of the human activities on the natural deep sea environment;
- An estimation of the thermal energy budget based on the hydrothermal fluids enthalpy and flow rate evaluations.

It is noteworthy to consider that, although the offshore geothermal energy exploration and exploitation have not yet been considered a feasible option, nowadays the technologies required for on-site geothermal exploitation and production of electric energy are already available, and can be adopted in view of the depth of seawater, about 600–800 m, and the minimum distance from the Italian coasts, less than 100 km. Presently, some projects are evaluated in European countries, for instance in Iceland, to develop offshore geothermal power plants to use high-temperature fluids lying along the mid-ocean ridges. Iceland is also developing the world's longest subsea power cable (about 1000 km), to export geothermal energy to Scotland. An eventual Marsili submarine power cable would "only" be around 150 km long.

Once the potentially exploitable geothermal energy of the Marsili seamount is well-constrained, that submarine volcano may become home to the world's first offshore geothermal power plant, potentially capable of doubling the current geothermal power output of Italy [45].

The increasing request for electrical power, the energy prices and the increasing know-how of the utilization of this resource makes the Marsili seamount an attractive scientific and industrial target. Several other seamounts of the Tyrrhenian sea, belonging to the same geological framework, share Marsili characteristics, among the most important: high heat-flow anomalies, relative shallow depth of the crest and rock porosity.

Acknowledgments

The Authors wish to thank the Eurobuilding S.p.A. for the fruitful cooperation during the data collection. The authors are indebted with Diego Paltrinieri for his comments and discussions during the development of the scientific activities.

Author Contributions

Patrizio Signanini and Paolo Favali were scientific coordinators of the geophysical projects; Mario L. Rainone and Sergio Rusi collected geophysical data during the 2006 scientific cruise and took care of the editing of the paper; Angelo De Santis e Francesco Italiano coordinated the geophysical and geochemical (respectively) data elaboration. All the authors cooperated to the writing of the paper.

Conflicts of Interest

The authors declare no conflict of interest.

References

1. Baker, E.T.; German, C.R.; Elderfield, H. Hydrothermal plumes over spreading-centre axes global distribution and geological inferences. In *Seafloor Hydrothermal Systems, Geophysical Monograph*; Humphris, S.E., Zierenberg, R.A., Mullineaux, L.S., Thomson, R.E., Eds.; American Geophysical Union: Washington, DC, USA, 1995; Geophysical Monograph Series, Volume 91, pp. 47–71.
2. Elderfield, H.; Schultz, A. Mid-ocean ridge hydrothermal fluxes and the chemical composition of the ocean. *Ann. Rev. Earth Planet. Sci.* **1996**, *24*, 191–224.
3. D'Alessandro, A.; D'Anna, G.; Luzio, D.; Mangano, G. The INGV new OBS/H: Analysis of the signals recorded at the Marsili submarine volcano. *J. Volc. Geoth. Res.* **2009**, *183*, 17–29.
4. Lupton, J.; de Ronde, C.; Sprovieri, M.; Baker, E.T.; Bruno, P.P.; Italiano, F.; Walker, S.; Faure, K.; Leybourne, M.; Britten, K.; *et al*. Active Hydrothermal Discharge on the Submarine Aeolian Arc: New Evidence from Water Column Observations. *J. Geophys. Res.* **2011**, *116*, B02102, doi:10.1029/2010JB007738.
5. Jannasch, H.W.; Mottl, M.J. Geo-microbiology of deep-sea hydrothermal vents. *Science* **1985**, *229*, 717–725.
6. Williams, D.L. Submarine geothermal resources. *J. Volc. Geoth. Res.* **1976**, *1*, 85–100.
7. Buonasorte, G.; Cameli, G.M.; Fiordelisi, A.; Parotto, M.; Perticone, I. Results of geothermal exploration in Central Italy (Latium-Campania). In Proceedings of the World Geothermal Congress, Florence, Italy, 18–31 May 1995; Volume 2, pp. 1293–1298.
8. Baldi, P.; Bertini, G.; Cameli, G.M.; Decandia, F.A.; Dini, I.; Lazzarotto, A.; Liotta, D. La tettonica distensiva post-collisionale nell'Area Geotermica di Larderello (Toscana meridionale). *Stud. Geol. Camerti* **1994**, *1*, 183–193.
9. Batini, F.; Brogi, A.; Lazzarotto, A.; Liotta, D.; Pandeli, E. Geological features of Larderello-Travale and Mt. Amiata geothermal areas (southern Tuscany, Italy). *Episodes* **2003**, *26*, 239–244.
10. Bertini, G.; Cappetti, G.; Fiordelisi, A. Characteristics of geothermal fields in Italy. *Giornale di Geologia Applicata* **2005**, *1*, 247–254.
11. Della Vedova, B.; Bellani, S.; Pellis, G.; Squarci, P. Deep temperatures and surface heat flow distribution. In *Anatomy of an Orogen: The Apennines and Adjacent Mediterranean Basin*; Vai, G.B., Martini, I.P., Eds.; Kluwer Academic Publishers: Dordrecht, The Netherlands, 2001; pp. 65–76.
12. Mongelli, F.; Zito, G.; de Lorenzo, S.; Doglioni, C. Geodynamic interpretation of the heat-flow in the Tyrrhenian Sea. *Mem. Descr. Carta. Geol. Ital.* **2004**, *LXIV*, 71–82.
13. Bertani, R. World geothermal generation in 2007. *GHC Bull.* **2007**, 8–19.
14. Marani, M.P.; Gamberi, F. Distribution and nature of submarine volcanic landforms in the Tyrrhenian Sea: The arc vs the back-arc. *Mem. Descr. Carta. Geol. Ital.* **2004**, *LXIV*, 109–126.

15. Doglioni, C.; Innocenti, F.; Morellato, C.; Procaccianti, D.; Scrocca, D. On the Tyrrhenian sea opening. *Mem. Descr. Carta. Geol. Ital.* **2004**, *LXIV*, 147–164.
16. Rosenbaum, G.; Lister, G.S. Neogene and Quaternary rollback evolution of the Tyrrhenian Sea, the Apennines, and the Sicilian Maghrebides. *Tectonics* **2004**, *23*, TC1013, doi:10.1029/2003TC001518.
17. Barberi, F.; Bizouard, H.; Capaldi, G.; Ferrara, G.; Gasparini, P.; Innocenti, F.; Joron, J.L.; Lambert, B.; Treuil, M.; Allegrè, C. Age and nature of basalts from the Tyrrhenian Abyssal Plain. In: *Initial Reports of the Deep-Sea Drilling Project*; Kenneth, H.J., Montadert, L., Bernoulli, D., Bizon, G., Cita, M., Erickson, A., Fabricius, F., Garrison, R.E., Kidd, R.B., Mélières, F., Müller, C., Wright, R.C., Eds.; IODP, 1978; doi:10.2973/dsdp.proc.42-1.1978, Publication date: May 2007, pp. 509–514. Available online: http://www.deepseadrilling.org/42_1/volume/dsdp42pt1_18.pdf (accessed on 25 June 2014).
18. Savelli, C. Late Oligocene to Recent episodes of magmatism in and around Tyrrhenian Sea: Implications for the processes of opening in a young inter-arc basin of intra-orogenic (Mediterranean) type. *Tectonophysics* **1988**, *146*, 163–181.
19. Beccaluva, L.; Coltorti, M.; Galassi, B.; Macciotta, G.; Siena, F. The Cainozoic calc-alkaline magmatism of the western Mediterranean and its geodynamic significance. *Boll. Geof. Teor. App.* **1994**, *36*, 293–308.
20. Selvaggi, G.; Chiarabba, C. Seismicity and P-wave velocity image of the Southern Tyrrhenian subduction zone. *Geophys. J. Int.* **1995**, *121*, 818–826.
21. Neri, G.; Caccamo, D.; Cocina, O.; Montalto, A. Geodynamic implications of earthquake data in the southern Tyrrhenian Sea. *Tectonophysics* **1996**, *258*, 233–249.
22. Favali, P.; Beranzoli, L.; Maramai, A. Review of the Tyrrhenian seismicity: How much is still to be known? *Mem. Descr. Carta. Geol. Ital.* **2004**, *LXIV*, 57–70.
23. Marani, M.P.; Gamberi, F. Structural framework of the Tyrrhenian Sea unveiled by seafloor morphology. *Mem. Descr. Carta. Geol. Ital.* **2004**, *LXIV*, 97–107.
24. Verzhbitskii, E.V. Heat flow and matter composition of the lithosphere of the world ocean. *Oceanology* **2007**, *47/4*, 564–570.
25. Steinmetz, L.; Ferrucci, F.; Hirn, A.; Morelli, C.; Nicolich, R. A 550-km-long Moho traverse in the Tyrrhenian Sea from OBS recorded P_n waves. *Geophys. Res. Lett.* **1983**, *10*, 428–431.
26. Locardi, E.; Nicolich, R. Geodinamica del Tirreno e dell'Appennino Centro Meridionale: La nuova carta della Moho. *Mem. Soc. Geol. Ital.* **1988**, *6*, 121–140.
27. Cella, F.; Fedi, M.; Florio, G.; Rapolla, A. Gravity modelling of the litho-asthenosphere system in the Central Mediterranean. *Tectonophysics* **1998**, *287*, 117–138.
28. Finetti, I.R. Innovative seismic highlights on the Mediterranean region. In *Geology of Italy, Special Volume of the Italian Geological Society*; Crescenti, U., D'Offizi, S., Merlino, S., Sacchi, L., Eds.; Società Geologica Italiana: Roma, Italy, 2004, pp. 131–140.
29. Vitale, S.; de Santis, A.; di Mauro, D.; Cafarella, L.; Palangio, P.; Beranzoli, L.; Favali, P. Geostar deep seafloor missions: Magnetic data analysis and 1D geoelectric structure underneath the Southern Tyrrhenian Sea. *Ann. Geophys.* **2009**, *52/1*, 57–63.
30. Turco, E.; Zuppetta, A. A kinematic model for the Plio-Quaternary evolution of the Tyrrhenian-Apenninic system: Implications for rifting processes and volcanism. *J. Volc. Geoth. Res.* **1998**, *82*, 1–18.

31. Pondrelli, S.; Piromallo, C.; Serpelloni, E. Convergence vs retreat in Southern Tyrrhenian Sea: Insights from kinematics. *Geophys. Res. Lett.* **2004**, *31*, doi:10.1029/2003GL019223.
32. Selli, R.; Lucchini, F.; Rossi, P.L.; Savelli, C.; del Monte, M. Dati geologici, petrochimici e radiometrici sui vulcani centro-tirrenici. *Gior. Geol.* **1977**, *42*, 221–246. (in Italian)
33. Savelli, C.; Gasparotto, G. Calc-alkaline magmatism and rifting of the deep-water volcano of Marsili (Aeolian back-arc, Tyrrhenian Sea). *Mar. Geol.* **1994**, *119*, 137–157.
34. Trua, T.; Serri, G.; Marani, M.; Renzulli, A.; Gamberi, F. Volcanological and petrological evolution of Marsili seamount (southern Tyrrhenian Sea). *J. Volc. Geoth. Res.* **2002**, *114*, 441–464.
35. Faggioni, O.; Pinna, E.; Savelli, C.; Schreider, A.A. Geomagnetism and age study of Tyrrhenian seamounts. *Geophys. J. Int.* **1995**, *123*, 915–930.
36. Marani, M.P.; Trua, T. Thermal constriction and slab tearing at the origin of a super-inflated spreading ridge: Marsili volcano (Tyrrhenian Sea*). J. Geophys. Res.* **2002**, *107*, doi:10.1029/2001JB000285.
37. Nicolosi, I.; Speranza, F.; Chiappini, M. Ultrafast oceanic spreading of the Marsili Basin, southern Tyrrhenian Sea: Evidence from magnetic anomaly analysis. *Geology* **2006**, *34/9*, 717–720.
38. Cocchi, L.; Caratori Tontini, F.; Muccini, F.; Marani, M.P.; Bortoluzzi, G.; Carmisciano, C. Chronology of the transition from a spreading ridge to an accretional seamount in the Marsili back-arc basin (Tyrrhenian Sea). *Terra Nova* **2009**, *21*, doi:10.111/j.1365-3121.2009.00891.x.
39. Dekov, V.M.; Savelli, C. Hydrothermal activity in the SE Tyrrhenian Sea: An overview of 30 years of research. *Mar. Geol.* **2004**, *204*, 161–185.
40. Italiano, F.; Caso, C.; Cavallo, A.; Favali, P.; Fu, C.; Iezzi, G.; Martelli, M.; Mollo, S.; Paltrinieri, D.; Paonita, A.; *et al*. Geochemical features of the gas phase extracted from sea-water and rocks of the Marsili seamount (Tyrrhenian sea, Italy): Implications for geothermal exploration projects. In Proceedings of the ICGG11, International Conference on Gas Geochemistry 2011, San Diego, CA, USA, 28 November–4 December 2011; Volume 67–68.
41. Lagmay, A.M.F.A.; Tengociang, A.M.P.; Marcos, H.B.; Pascua, C.S. A structural model for geothermal exploration in Ancestral Mount Bao, Leyte, Philippines. *J. Volc. Geoth. Res.* **2003**, *122*, 133–141.
42. Murton, B.J.; Parson, L.M. Segmentation, volcanism and deformation of oblique spreading centres: A quantitative study of the Reykjanes Ridge. *Tectonophysics* **1993**, *222*, 237–257.
43. McGuire, W.J. Volcano instability: A review of contemporary themes. In *Volcano Instability on the Earth and Other Planets*; Mc Guire, W.J., Jones, A.P., Neuberg, J., Eds.; *Geol. Soc. Lond. Spec. Publ.* **1996**, *110*, 1–23.
44. Blanco-Montenegro, I.; Nicolosi, I.; Pignatelli, A. Magnetic imaging of the feeding system of oceanic volcanic islands: El Hierro (Canary Islands). *Geophys. J. Int.* **2008**, *173*, 339–350.
45. Caso, C.; Signanini, P.; de Santis, A.; Favali, P.; Iezzi, G.; Marani, M.P.; Paltrinieri, D.; Rainone, M.L.; di Sabatino, B. Submarine geothermal systems in Southern Tyrrhenian Sea as future energy resource: The example of Marsili seamount. In Proceedings of the World Geothermal Congress 2010, Bali, Indonesia, 25–30 April 2010; pp. 1–9.
46. Italiano, F.; Bonfanti, P.; Ditta, M.; Petrini, R.; Slejko, F. Helium and carbon isotopes in the dissolved gases of Friuli region (NE Italy): Geochemical evidence of CO_2 production and degassing over a seismically active area. *Chem. Geol.* **2009**, *266*, 76–85, doi:10.1016/j.chemgeo.2009.05.022.

47. Italiano, F.; Sasmaz, A.; Yuce, G.; Okan, O. Thermal fluids along the East Anatolian Fault Zone (EAFZ): Geochemical features and relationships with the tectonic setting. *Chem. Geol.* **2013**, *339*, 103–114, doi:10.1016/j.chemgeo.2012.07.027.
48. Hildenbrand, T.G.; Tosenbaum, J.; Kauahikaua, J. Aeromagnetic study of the island of Hawaii. *J. Geophys. Res.* **1993**, *98*, 4099–4119.
49. Tivey, M. Fine-scale magnetic anomaly field over the southern Juan de Fuca Ridge: Axial magnetisation low and implications for crustal structure. *J. Geophys. Res.* **1994**, *99*, 4833–4855.
50. Irving, E. The Mid-Atlantic Ridge at 45° N. Oxidation and magnetic properties of basalt; Review and discussion. *Can. J. Earth Sci.* **1970**, *7*, 1528–1538.
51. Johnson, H.P.; Karsten, J.L.; Vine, F.J.; Smith, G.C.; Schonharting, G. A low-level magnetic survey over a massive sulfide ore body in the Troodos ophiolite complex, Cyprus. *Mar. Tech. Soc. J.* **1982**, *16*, 76–79.
52. Uchupi, E.; Ballard, R.D. Evidence of hydrothermal activity on Marsili Seamount, Tyrrhenian Basin. *Deep-Sea Res. Part A*, *Oceanogr. Res. Pap.* **1989**, *36*, 1443–1448.
53. Caratori Tontini, F.; Cocchi, L.; Muccini, F.; Carmisciano, C.; Marani, M.P.; Bonatti, E.; Ligi, M.; Boschi, E. Potential-field modeling of collapse-prone submarine volcanoes in southern Tyrrhenian Sea (Italy). *Geophys. Res. Lett.* **2010**, *37*, doi:10.1029/2009GL041757,2010.
54. Wallace, P.J. Volatiles in subduction zones magmas: Concentrations and fluxed based on melt inclusion and volcanic gas data. *J. Volc. Geoth. Res.* **2005**, *114*, 441–464.
55. Kieffer, S.W. Seismicity at Old Faithful Geyser: An isolated source of geothermal noise and possible analogue of volcanic seismicity. *J. Volc. Geoth. Res.* **1984**, *22*, 59–95.
56. Crone, T.J.; Wilcock, W.S.D.; Barclay, A.; Parsons, J.D. The sound generated by mid-ocean ridge black smoker hydrothermal vents. *PLoS One* **2006**, *1*, doi:10.1371/journal.pone.0000133.
57. Legaz, A.; Revil, A.; Roux, P.; Vandemeulebrouck, J.; Gouèdard, P.; Hurst, T.; Bolève, A. Self-potential and passive seismic monitoring of hydrothermal activity: A case study at Iodine Pool, Waiomangu geothermal valley, New Zealand. *J. Volc. Geoth. Res.* **2009**, *179*, 11–18.
58. Chouet, B. Long-period volcano seismicity: Its source and use in eruption forecasting. *Nature* **1996**, *380*, 309–316.
59. Kumagai, H.; Chouet, B. The complex frequencies of long-period seismic events as probes of fluid composition beneath volcanoes. *Geophys. J. Int.* **1999**, *138*, F7–F12.
60. Sgroi, T.; Montuori, C.; Agrusta, R.; Favali, P. Low-frequency seismic signals recorded by OBS at Stromboli volcano (Southern Tyrrhenian Sea). *Geophys. Res. Lett.* **2009**, *36*, L04305, doi:10.1029/2008GL036477.
61. Iezzi, G.; Caso, C.; Ventura, G.; Vallefuoco, M.; Cavallo, A.; Behrens, H.; Mollo, S.; Paltrinieri, D.; Signanini, P.; Vetere, F. First documented deep submarine explosive eruptions at the Marsili Seamount (Tyrrhenian Sea, Italy): A case of historical volcanism in the Mediterranean Sea. *Gondwana. Res*. **2014**, *25*, 764–774.
62. Eurobuilding, Marsili Project. Available online: http://www.eurobuilding.it/marsiliproject/ (accessed on 10 March 2014).
63. Armani, F.B.; Paltrinieri, D. Perspectives of offshore geothermal energy in Italy. *EPJ Web Conf.* **2013**, *54*, 02001, doi:10.1051/epjconf/20135402001.

64. Beranzoli, L.; Ciafardini, A.; Cianchini, G.; de Caro, M.; de Santis, A.; Favali, P.; Frugoni, F.; Marinaro, G.; Monna, S.; Montuori, C.; *et al*. A first insight in the Marsili volcanic seamount (Tyrrhenian Sea): Results from ORION-GEOSTAR3 experiment. In: *Seafloor Observatories: A New Vision of the Earth from the Abyss*; Favali, P., Beranzoli, L., de Santis, A., Eds.; Springer-Praxis Publishing: Amsterdam, The Netherlands, 2014; ISBN:978-3-642-11373-4 (in press).
65. Favali, P.; Beranzoli, L.; de Santis, A. *Seafloor Observatories: A New Vision of the Earth from the Abyss*; Favali, P., Beranzoli, L., de Santis, A., Eds.; Springer-Praxis Publishing: Amsterdam, The Netherlands, 2014; ISBN:978-3-642-11373-4.